


Mesenchymal Stem Cells Derived from Wharton's Jelly Can Differentiate into Schwann Cell-Like Cells and Promote Peripheral Nerve Regeneration in Acellular Nerve Grafts

Soon Jin Choi¹ · Suk Young Park¹ · Young Ho Shin² · Seung-Ho Heo³ · Kang-Hyun Kim³ · Hyo In Lee³ · Jae Kwang Kim^{1,2} 

Received: 7 August 2020 / Revised: 8 December 2020 / Accepted: 18 December 2020 / Published online: 30 January 2021
© The Korean Tissue Engineering and Regenerative Medicine Society 2021

Abstract

BACKGROUND: Schwann cells (SCs) secrete neurotrophic factors and provide structural support and guidance during axonal regeneration. However, nearby nerves may be damaged to obtain primary SCs, and there is a lack of nervous tissue donors. We investigated the potential of Wharton's Jelly-derived mesenchymal stem cells (WJ-MSCs) in differentiating into Schwann cell-like cells (WJ-SCLCs) as an alternative to SCs. We also examined whether implantation of WJ-SCLCs-laden acellular nerve grafts (ANGs) are effective in inducing functional recovery and nerve regeneration in an animal model of peripheral nerve injury.

METHODS: The differentiation of WJ-MSCs into WJ-SCLCs was determined by analyzing SC-specific markers. The secretion of neurotrophic factors was assessed by the Neuro Discovery antibody array. Neurite outgrowth and myelination of axons were found in a co-culture system involving motor neuron cell lines. The effects of ANGs on repairing sciatic nerves were evaluated using video gait angle test, isometric tetanic force analysis, and toluidine blue staining.

RESULTS: Compared with undifferentiated WJ-MSCs, WJ-SCLCs showed higher expression levels of SC-specific markers such as S100 β , GFAP, KROX20, and NGFR. WJ-SCLCs also showed higher secreted amounts of brain-derived neurotrophic factor, glial cell-derived neurotrophic factor, and granulocyte-colony stimulating factor than did WJ-MSCs. WJ-SCLCs effectively promoted the outgrowth and myelination of neurites in motor neuron cells, and WJ-SCLCs laden ANGs significantly facilitated peripheral nerve regeneration in an animal model of sciatic nerve injury.

CONCLUSION: WJ-MSCs were readily differentiated into WJ-SCLCs, which effectively promoted the regeneration of peripheral nerves. Transplantation of WJ-SCLCs with ANGs might be useful for assisting peripheral nerve regeneration.

Keywords Acellular nerve grafts · Schwann cell-like cells · Wharton's jelly-derived mesenchymal stem cells · Nerve repair

1 Introduction

Injured peripheral nerves are generally difficult to regenerate and often result in long-lasting neural deficits [1–3]. Although nerve autografts are considered as the gold standard for repairing nerve injuries, the scarcity of donor tissues and mismatches between the graft size and the injury site limit a wide application of nerve autografts [4, 5]. To overcome these limitations, alternative methods including acellular nerve allografts (ANGs) and synthetic conduits have been developed. Particularly, ANGs induce

✉ Jae Kwang Kim
orth4535@gmail.com

¹ Asan Peripheral Nerve Regeneration Lab Institute for Life Sciences, Seoul, South Korea

² Department of Orthopedic Surgery, Asan Medical Center, University of Ulsan College of Medicine, 88, Olympic Road 43-gil, Songpa-gu, Seoul 05505, South Korea

³ Convergence Medicine Research Center, Asan Medical Center, Seoul, South Korea

minimal immunological responses because antigenic cellular components are removed in the preparation process of ANGs [6]. Unlike nerve conduits, ANGs retain the microstructure of extracellular matrix proteins and are thus effective in supporting the regeneration of nerves [7, 8]. However, the use of ANGs alone has limits in the length of axons that can be regenerated; therefore, neuronal support cells such as Schwann cells (SCs) are needed for sufficient proliferation of axons [9–11].

SCs in peripheral nerve tissues ensheath the nerve fibers, carry nerve signals along the axons, provide structural support, and guide axonal regeneration [12, 13]. Furthermore, SCs secrete a variety of cytokines, neurotrophic factors, and extracellular matrix molecules to provide structural support and guidance in the process of axon regeneration [14]. As such, SCs have been suggested as a viable source of cells for use in transplantation for inducing functional recovery of peripheral nerves. However, obtaining a sufficient amount of SCs from neural biopsies often entails damaging nearby functional nerves. In addition, culturing primary SCs to obtain a sufficient amount of cells is technically challenging. Therefore, it is necessary to develop alternative cell sources that are easily accessible and show high capabilities for differentiation and self-renewal.

Mesenchymal stem cells (MSCs), which are multipotent stem cells derived from various tissues, have shown promising results for use in tissue engineering [15]. MSCs can be derived from bone marrows (BM-MSCs), skin cells, adipose tissues, and tonsils; importantly, MSCs can be used to differentiate into neurons and glial cells, and attempts have been made to differentiate MSCs into SCs as well [16–19]. Although BM-MSCs have been extensively explored in terms of their potential to differentiate into SCs, they have limited clinical application because of the invasive procedure required for their isolation and the low yield; moreover, the differentiation and proliferation abilities of BM-MSCs were shown to decrease with the age of the donor [20]. In this aspect, Wharton's jelly MSCs (WJ-MSCs) isolated from human umbilical cords have multiple advantages over adult MSCs in that WJ-MSCs can be obtained in a non-invasive manner by collecting discarded tissues from umbilical cords and that WJ-MSCs have a high proliferation rate. Furthermore, WJ-MSCs have higher expression levels of pluripotency markers than do MSCs of other origins [21–23].

Despite the advantages of WJ-MSCs, studies on the differentiation of WJ-MSCs into SC-like cells (SCLCs) are still insufficient. Furthermore, the application of WJ-SCLCs to ANGs for peripheral nerve regeneration *in vivo* has yet to be tested. Therefore, in this study, we demonstrated that WJ-MSCs can differentiate into WJ-SCLCs by using evidence from Western Blot, real-time PCR analysis,

immunofluorescence staining, and antibody array. The WJ-SCLCs were co-cultured with NSC34 motor neuron cells to assess the outgrowth of neurites. Finally, we investigated the potential of WJ-SCLCs as an alternative of autologous SCs by transplanting ANGs laden with WJ-SCLCs and analyzing the degree of functional recovery and nerve regeneration.

2 Materials and methods

2.1 Isolation and culture of human MSCs

WJ-MSCs were isolated from human umbilical cords and cultured *in vitro* as described previously [24]. In brief, umbilical cords were washed with PBS and cut into 0.5- to 1.0-cm pieces; to remove blood vessels, each piece was cut longitudinally. The matrix was minced and transferred to culture dishes (100-mm; SPL Life Science, Pocheon, Korea). The WJ-MSCs were cultured in minimum essential medium- α (Thermo Fisher Scientific, Waltham, MA, USA) supplemented with $1 \times$ antibiotic/antimycotic solution (Gibco BRL, Gaithersburg, MD, USA) and 10% fetal bovine serum for 7 days at 37 °C in 5% CO₂. When the WJ-MSCs reached 80% confluency, the cells were replated at a split ratio of 1:3.

2.2 Characterization of MSCs

For analysis with flow cytometry, WJ-MSCs were trypsinized, washed, and resuspended in PBS with 1 mM EDTA and 2% FBS. The resuspended cells were then incubated with MSC-specific markers at 4 °C for 30 min. Fluorescein isothiocyanate (FITC)-conjugated mouse anti-human CD105 antibody and phycoerythrin (PE)-conjugated mouse anti-human CD73 antibody were purchased from BD Biosciences (San Jose, CA, USA). PE-conjugated mouse anti-human CD34 and CD45 antibodies were purchased from BD PharMingen™ (San Jose, CA, USA). BD FACS Canto™ II Flow Cytometer and FACSDIVA software (v6.1.3; BD Biosciences) were used for cell surface marker analysis.

2.3 Differentiation into Schwann cell-like cells

The technique reported by Xu et al. [25] was used to induce the differentiation of WJ-MSCs into WJ-SCLCs. Briefly, WJ-MSCs were harvested, plated in plastic dishes at a density of 2.8×10^3 cells/cm², and treated with 1 mM β -mercaptoethanol (β -ME; Sigma–Aldrich, St. Loise, MO, USA) for 24 h in α -MEM. Then, the medium was replaced with α -MEM containing 10% FBS and 35 ng/ml all-trans-retinoic acid (RA; Sigma–Aldrich) and incubated for

3 days. The cells were then washed with PBS and cultured in α -MEM containing 10% FBS, 400 ng/ml recombinant human heregulin (HRG)- β 1, 10 ng/ml recombinant human basic fibroblast growth factor (bFGF), 10 μ M forskolin (FSK), and 5 ng/ml recombinant human platelet-derived growth factor (PDGF) for 10 days.

2.4 Quantitative real-time polymerase chain reaction

TRIzol (Thermo Fisher Scientific) was used to extract total RNA from WJ-MSCs and WJ-SCLCs. Revert Aid First Strand cDNA Synthesis Kit (Thermo Scientific) was used to synthesize cDNA from 1 μ g of total RNA. Power SYBR® Green PCR Master Mix Kits and the ABI7500 fast real-time PCR system (Applied Biosystems/Thermo Fisher Scientific) were used to quantify the amount of mRNA. All experiments were performed in triplicates and independently repeated more than 3 times. The following primers were used: S100 β (forward, GGA GAC GGC GAA TGT GAC TT; reverse, GAA CTC GTG GCA GGC AGT AGT AA), GFAP (forward, GAC AGC AGG TCC ATG TA; reverse, GTT GCT GGA CGC CAT TGC), NGFR (forward, GAA GCT TCT CAA CGG CTC TG; reverse, CTG CAC AGA CTC TCC ACG AG), KROX20 (forward, GGA GGG CAA AAG GAG ATA CC; reverse, CACAACCTG GAGACCCAACCT), MBP (forward, CAC ATT TGT TCC CTG CAC AC; reverse, GAC TTC AGG CAT TGC TCA CA), and β -ACTIN (forward, AGA GCT ACG AGC TGC CTG AC; reverse, AGC ACT GTG TTG GCG TAC AG). The comparative C_t method ($2^{-\Delta\Delta C_t}$) [26] was used to analyze the relative amount of gene expression.

2.5 Western Blot analysis

Western blot analysis was performed according to a previously described protocol [27]. Proteins in WJ-MSCs and WJ-SCLCs were extracted with RIPA lysis buffer (CST, USA) containing Protease and Phosphatase Inhibitor Cocktail solution (Thermo Fisher Scientific). The following antibodies were used: anti-S100 β (Cell Signaling Technology, Beverly, MA, USA), anti-GFAP (Millipore, Billerica, MA, USA), anti-p75NGFR (Cell signaling Technology, Beverly, MA, USA), anti- α -tubulin (Millipore, Billerica, MA, USA) antibodies.

2.6 Immunofluorescence staining

WJ-MSCs and WJ-SCLCs were seeded into chamber slide dishes. After treatment with 4% paraformaldehyde for 10 min and 0.2% Triton X-100 for 10 min, the cells were incubated with anti-GFAP (Millipore, Billerica, MA,

USA), anti-NGFR, and anti-S100 β (1:200, Abcam, Cambridge, UK) antibodies at 4 °C for overnight. Then, the cells were incubated with Alexa Fluor 488, 594-labeled goat anti-mouse or rabbit secondary antibodies (Invitrogen Japan, Tokyo, Japan). DAPI was used for nuclei staining. Images were obtained with a confocal microscope (Carl Zeiss Micro Imaging, Inc., Thornwood, NY, USA).

2.7 Neuro Discovery array

Neuro Discovery array arrays were performed using Ray Bio C-Series Human Neuro Discover ArrayC1 (AAH-NEUF-1-8; Ray Biotech, Norcross, GA, USA) according to the manufacturer's instructions. After 3 days, conditioned medium (CM) was collected and concentrated using Amicon Ultra-15 (Merk, Darmstadt, Germany). After the membranes were blocked with blocking buffer, 1 ml of CM was added and incubated at 4 °C overnight. The resulting immunoreactivity was quantified in Image J (National Institutes of Health, Bethesda, MD, USA).

2.8 WJ-SCLCs and mouse NSC34 co-culture

To evaluate the degree of myelination in co-cultures, we used the technique reported by Takaku et al. [28]. NSC34 cells (mouse motor neuron cell line) were trypsinized and seeded onto collagen-coated chamber slides at a density of $3 \times 10^3/\text{cm}^2$. The cells were maintained for 5 days in DMEM/F12 supplemented with 1% FBS, 1% MEM NEAA (Thermo Fisher Scientific), and 10 ng/ml recombinant brain-derived neurotrophic factor (BDNF) (Peprotech, Cranbury, NJ, USA). When the majority of NSC-34 cells revealed neurite elongation in phase-contrast microscopy, the cells were incubated for 12–16 h with DMEM/F12 supplemented with 5% FBS and 1 μ g/ml mitomycin C (Sigma Aldrich). The NSC-34 cells were then co-cultured with WJ-SCLCs cells that were detached from the dishes and suspended in DMEM/5% FBS at a density of $1 \times 10^5/\text{ml}$. The ratio of NSC34 to SCLCs was between 1:7 to 1:10. The co-cultured cells were maintained in media containing 10 ng/ml recombinant ciliary neurotrophic factor (CNTF; Peprotech), 10 ng/ml BDNF, 50 μ g/ml L-ascorbic acid (Sigma-Aldrich), and 5% FBS. All culture medium was replaced three times per week. Fluorescence of the culture was visualized under a confocal microscope (Carl Zeiss LSM 700, Göttingen, Germany). To visualize the myelination of NSC-34 cells, the co-cultured cells were fixed with 4% paraformaldehyde and co-stained with anti- β III tubulin (1:200, Abcam) and anti-MBP (1:200, Abcam). Zen 3.0 software (Carl Zeiss Microscopy, Göttingen, Germany) was used to measure the lengths of the axons.

2.9 Preparation of acellular nerve grafts

To prepare ANGs, we harvested 14 sciatic nerve segments (10-mm in length) from 7 male Sprague–Dawley rats (7–8 weeks old) weighing 250–350 g (Orient Bio Inc., Seongnam, Korea). After isoflurane induction, the rats were euthanized by CO₂ inhalation. Under aseptic conditions, the nerve segments were removed, cleared of external fat and connective tissue, and immediately placed in sterile distilled water. All segments were decellularized using the protocol described by Shin et al. [29]. Briefly, the samples were treated with detergents, including CHAPS, aprotinin, and nuclease solutions. The decellularized nerves were then washed with PBS to remove any residual reagents and stored in PBS at 4 °C until use. All solutions were autoclaved or filter-sterilized before use.

2.10 Surgical procedure

Sprague–Dawley rats were randomly assigned into either the control (CTL) group (only received ANGs; $n = 7$) or the experiment group (received WJ-SCLCs-laden ANGs; $n = 7$). The structure of the ANGs can be damaged during injection via syringes, thereby leading to limited accumulation of seed cells [30]. To solve this problem, WJ-SCLCs were mixed with fibrin glue and dropped on the ANGs, which were utilized to repair the 6-mm nerve defects. After anesthetization, the left surgical sites were shaved and sterilized with 75% ethanol. Skin was excised along the femoral axis, and the sciatic nerve was exposed by separating the thigh muscles. The left sciatic nerves were severed in the middle of the thigh near the occlusive muscle and contracted. The nerve stumps were transected and 6 mm of the nerve was removed. ANGs or WJ-SCLCs-laden ANGs were used to bridge the stumps of the sciatic nerve gaps. All sutures were performed under a microscope using 9-0 nylon (Ethicon, Somerville, NY, USA). The skin incisions were clamped shut with wound clips. For recovery from anesthesia following the surgery, the rats were placed under a warming light.

2.11 Assessment of functional recovery *in vivo*

2.11.1 Video gait angle analysis

The movement of the ankles in rats during walking is affected by recovery, and the angle measured at the toe-off phase is known to be related to sciatic nerve recovery [31]. The ankle angles at the toe-off phase at post-operative weeks 4, 8, and 12 were measured to assess the functional recovery. For this test, a walking track (1 m length, 10 cm width, and 10 730 cm height) was built. During the test, video recording was acquired at a distance of 1 m with a

digital camera (Canon SX HS, Canon, Tokyo, Japan) and corrected to reduce optical distortion. Records were repeated until 3 satisfactory trials were obtained per rat. The angle of the ankle in the toe-off phase was measured at maximal plantar flexion in the experimental lateral ankle joint. After manually identifying the foot and leg segments in the video frames, the angles of the ankle at toe-off were displayed in degrees.

2.11.2 Isometric tetanic force measurement

The maximum isometric tetanic force at post-operative 16 weeks was measured according to a previously described protocol [29]. In brief, the skin in front of the ankle was incised to expose and distally transect the tibialis anterior (TA) tendon. Stimuli were generated using a bipolar stimulator (Grass Instrument Corp., Quincy, MA, USA) and processed with the LabVIEW software (National Instruments, Austin, TX, USA). The strength of the muscles was normalized using data from the other side and reported as a percentage of the data from the other side.

2.11.3 Analysis of toluidine blue staining

The implanted sciatic nerves were harvested by including the distal sites, and 2.5% glutaraldehyde solution was used for fixation. The harvested nerves were further fixed in 1% osmium tetroxide, ethanol-dehydrated, and embedded in EPON resin (Miller-Stephenson Chemical C, Sylmer, CA, USA). For visualization of myelin with light microscopy, cross-sections (1- μ m thick) were stained with toluidine blue. Images of non-overlapping fields (400 \times magnification) were obtained using unbiased random sampling. Total axon count and axonal area of the nerve fiber were calculated with the ImageJ software (National Institutes of Health).

2.12 Statistical analysis

All experiments were repeated five times or more. Values are presented as mean \pm SEM. P values < 0.05 were considered statistically significant. All statistical analyses were performed using the Student's t -test using GraphPad Prism v5 (GraphPad Software, Inc., San Diego, CA, USA).

3 Results

3.1 Identification of MSCs by Flow Cytometry

We first isolated and cultured WJ-MSCs of neonatal umbilical cord tissue, then passaged these cells. Flow cytometry was used to investigate the mesodermal

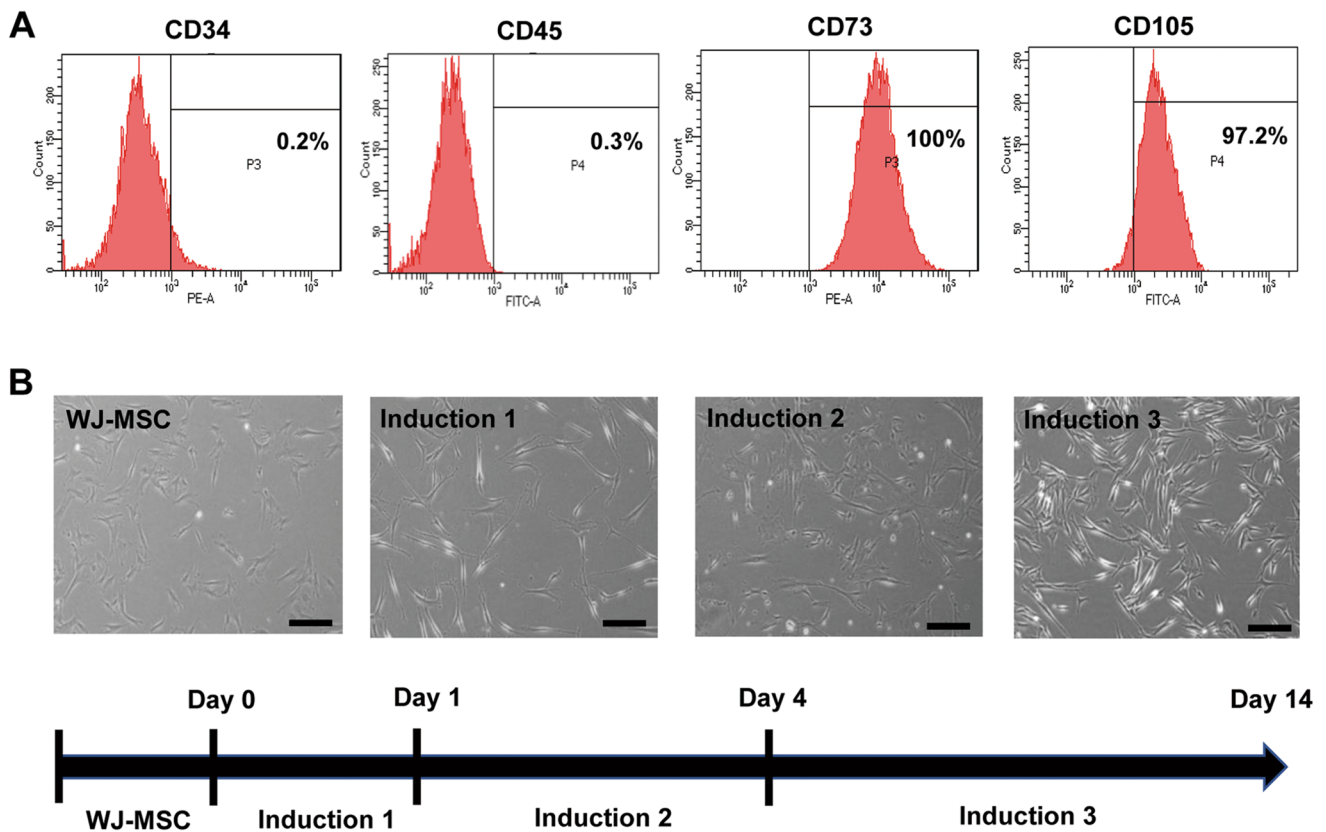


Fig. 1 Identification of human WJ-MSCs and the schematic design for the differentiation of WJ-MSCs into WJ-SCLCs. **A** Flow cytometry of WJ-MSCs for CD34, CD45, CD73, and CD105. **B** Light microscopy images of the MSCs during differentiation, which was

differentiation ability of WJ-MSCs and the cell surface markers thereof. Flow cytometric analysis showed that WJ-MSCs expressed typical MSC surface markers (e.g., CD73 and CD105) and did not express CD34 and CD45. Thus, WJ-MSCs showed that MSCs have the potential for differentiation (Fig. 1A).

3.2 Differentiation and characterization of WJ-SCLCs

Phenotypic changes were observed after the WJ-MSCs were differentiated into WJ-SCLCs. Whereas WJ-MSCs had a fibroblast-like morphology, the differentiated WJ-SCLCs became morphologically more similar to primary SCs and exhibited a narrow spindle-like shape with a bipolar or tripolar structure as the induction period was prolonged. Differentiation was induced in three stages with β -ME, retinoic acid, and growth factors (i.e., FGF-2, neuregulin 1 β , forskolin, PDGF) (Fig. 1B).

To evaluate the differentiation potential of WJ-SCLCs, the mRNA levels of representative genes related to SCs were compared between WJ-MSCs and WJ-SCLCs. Key cellular markers of SCs including S100 calcium-binding

induced in three steps: induction 1 (1 mM β -ME), induction 2 (35 ng/ml retinoic acid), and induction 3 (10 μ M forskolin, 400 ng/ml heregulin- β , 5 ng/ml PDGF, and 10 ng/ml β -FGF). Scale bar = 50 μ m

protein (S100 β), nerve growth factor receptor (NGFR), and glial fibrillary acidic protein (GFAP) [32] were analyzed. The mRNA levels of GFAP, S100 β , and NGFR were significantly higher in the differentiated SCLCs ($p < 0.05$). Differentiated SCLCs showed a significantly higher expression of KROX20, which suppresses the immature state and induces myelination [33], while showing a decreased expression of myelin basic protein (MBP), a specific marker of the mature stage of SC development [34] (Fig. 2A). Western Blot analysis and immunofluorescence staining using antibodies against GFAP, S100 β , and NGFR were performed before and after the differentiation of WJ-SCLCs. The protein expression levels of GFAP, NGFR, and S100 β were notably increased after differentiation into SCLCs (Fig. 2B, C). These data show that human WJ-MSCs are able to differentiate into WJ-SCLCs.

3.3 CM cytokine array

We used the human Neuro Discovery array to determine the level of secreted neurotrophic factors. The signal intensities of BDNF, granulocyte-colony stimulating factor (GCSF), and glial cell-derived neurotrophic factor (GDNF)

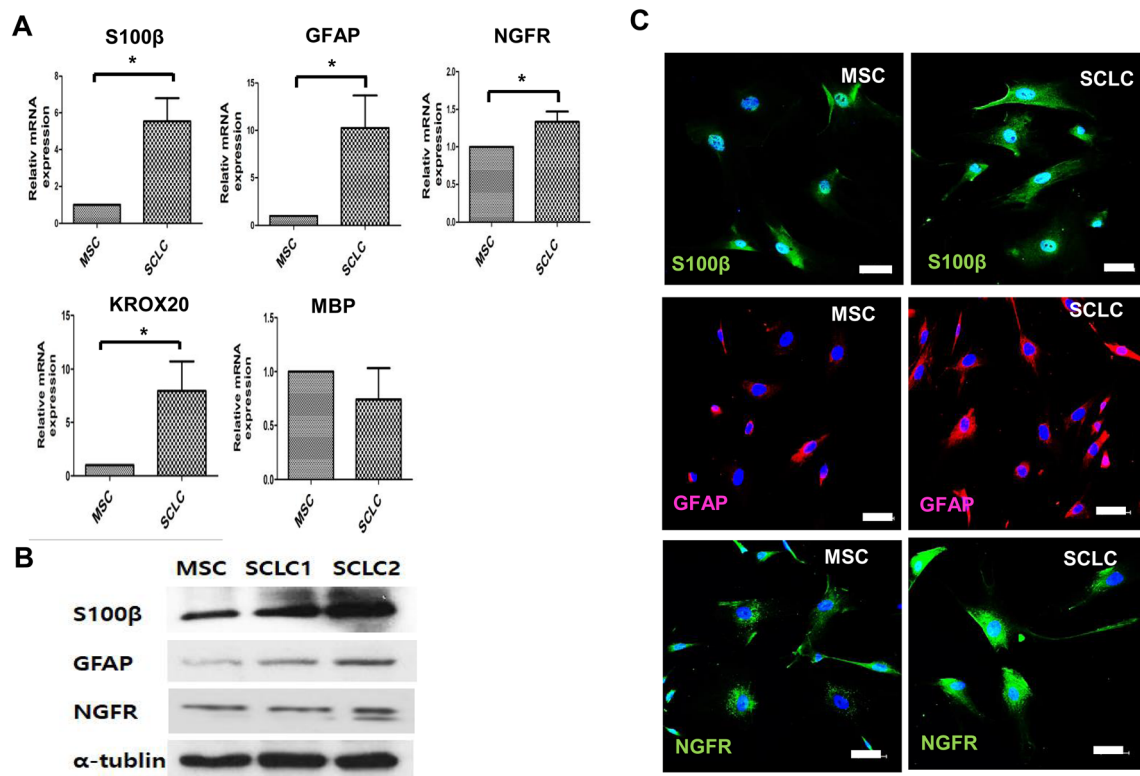


Fig. 2 Expression of SC markers in WJ-MSCs and WJ-SCLCs. **A** RT-qPCR analyses on S-100β, GFAP, NGFR, KROX20, and MBP in WJ-MSCs and SCLCs. Expression levels were normalized against that of GAPDH. **B** Western blot analysis of S-100β, GFAP, and NGFR in WJ-MSCs and SCLCs. **C** Immunocytochemical staining for

S100β (blue, DAPI; green, S100β), GFAP (blue, DAPI; red, GFAP), and NGFR (blue, DAPI; green, NGFR) before and after differentiation into SCLCs. Data are presented as mean \pm SEM of at least three experiments. Statistical analysis was performed using Student's *t*-test (* $p < 0.05$). Scale bar = 50 μ m

were significantly higher in WJ-SCLCs-CM compared with control (WJ-MSCs-CM) ($p < 0.05$) (Fig. 3A). The quantified results are shown in mean \pm standard error ($n = 3$) (Fig. 3B).

3.4 Neurite outgrowth of WJ-SCLCs from WJ-MSCs

The ability of WJ-SCLCs in promoting the outgrowth of neurites was examined by observing their interaction with NSC34 cells (motor neuron-like cell line) [28]. Images of co-cultures after 7 days were used to quantify the length of the longest neurites (Fig. 4A, B). Control cultures (NSC34 cells grown alone) and NSC34 cells seeded with WJ-MSCs or WJ-SCLCs were compared. The longest length of neurites in control cultures and NSC34 cells seeded with WJ-MSCs or WJ-SCLCs were $119.7 \pm 9.31 \mu\text{m}$, $158.0 \pm 12.19 \mu\text{m}$ ($p < 0.05$ vs. control), and $209.4 \pm 16.93 \mu\text{m}$ ($p < 0.001$ vs. control), respectively. In order to confirm myelination in the co-culture model of WJ-SCLCs and NSC34 cells, we co-stained the cells with β 3-tubulin and MBP. Whereas MBP positive axons were not observed at 10 days of co-culture, it

was detected with β 3-tubulin in the axons of the co-culture at 20 days (Fig. 4C).

3.5 Assessment of functional recovery *in vivo*

3.5.1 Video gait angle analysis

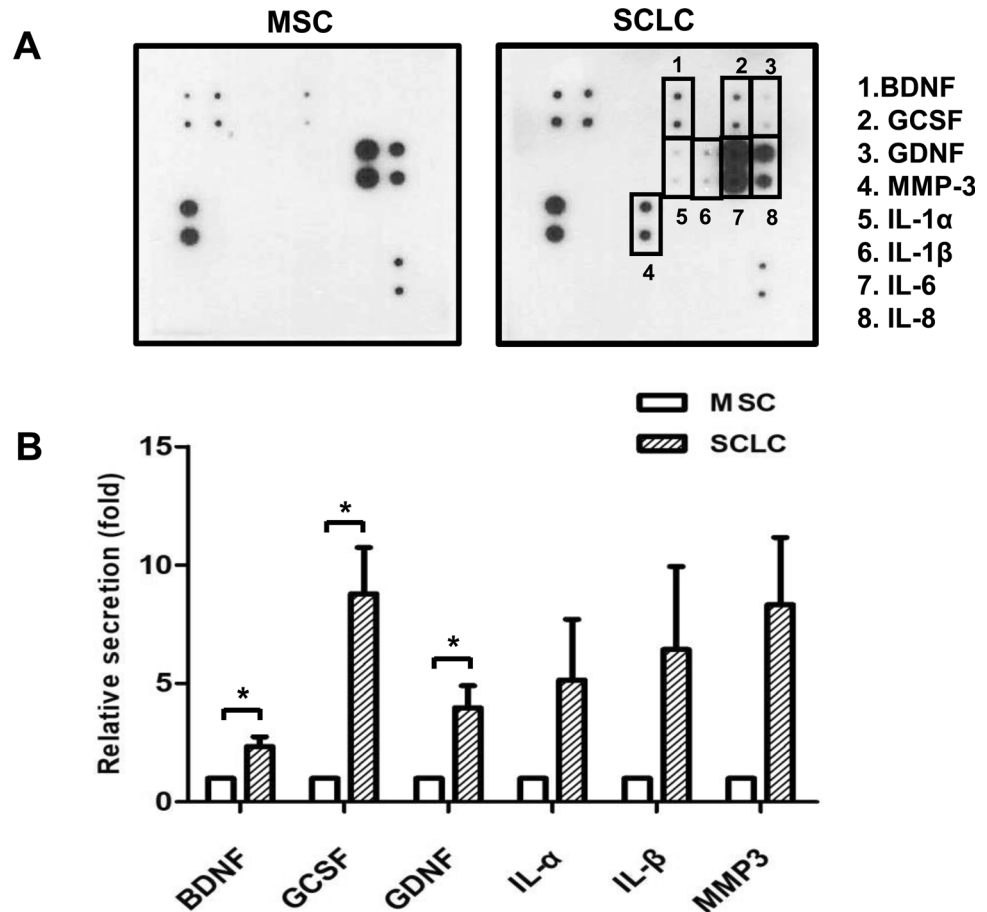
The video gait angle was analyzed to evaluate the effects of WJ-SCLCs on sciatic peripheral nerve recovery as the toe-off phase gait is strongly correlated with sciatic nerve regeneration [31]. The mean ankle angles at the toe-off phase of the control group (ANGs only) at 4, 8, and 12 weeks were $64.2^\circ \pm 1.1^\circ$, $71.2^\circ \pm 2.8^\circ$, and $76.0^\circ \pm 3.7^\circ$, respectively. The WJ-SCLCs group (SCLCs laden-ANGs) showed higher ankle angles at 4, 8, and 12 weeks at $76.0^\circ \pm 3.7^\circ$ ($p < 0.05$ vs. control), $75.8^\circ \pm 3.0^\circ$, and $85.5^\circ \pm 2.4^\circ$ ($p < 0.001$ vs. control), respectively (Fig. 5A).

3.5.2 Isometric tetanic force measurement

The measurement of tetanic force is an invaluable tool for assessing muscle strength after nerve repair or injury [35].

Fig. 3 Secreted growth factors in WJ-MSCs and SCLCs.

A Neuro Discovery array analysis for the secretion of growth factors in the conditioned medium derived from WJ-MSCs and SCLCs. **B** Levels of brain-derived neurotrophic factor (BDNF), glial cell line-derived neurotrophic factor (GDNF), and granulocyte colony-stimulating factor (G-CSF) in WJ-MSCs-CM compared with those in WJ-SCLCs CM. Results are shown as mean \pm SEM ($n = 4$). Statistical analysis was performed using Student's *t*-test ($*p < 0.05$)



At 16 weeks, the percentage recovery of the isometric tetanic force in the TA of the control group (ANGs only) and the WJ-SCLCs group (SCLCs laden-ANGs) were $23.4\% \pm 7.1\%$ and $40.6\% \pm 13.1\%$, respectively ($p < 0.05$; Fig. 5B).

3.5.3 Analysis of toluidine blue staining

Sciatic nerve axonal regeneration in each group was directly examined at 16 weeks postoperatively using toluidine blue staining. The histological structures of axons and nerve fibers are shown in Fig. 5C. The total number of myelinated axons in the control group and the WJ-SCLCs group (SCLCs laden-ANGs) was 895.0 ± 78.6 and 1235.0 ± 51.5 , respectively ($p < 0.05$; Fig. 5D). The total axonal area in the control group and the WJ-SCLCs group was $10,490 \pm 1033$ and $14,390 \pm 602.9$, respectively ($p < 0.05$; Fig. 5E).

4 Discussion

In this study, we investigated the ability of WJ-SCLCs for promoting nerve regeneration in ANGs. Previous studies have demonstrated that MSCs can be used for the regeneration of peripheral nerves, and that SCLCs derived from BM-MSCs and adipose-derived stem cells (ASCs) could improve peripheral nerve regeneration [32, 36]. ASCs have been reported to be more effective than BM-MSCs due to their low invasiveness and higher yield [37]. However, a recent study using a mouse sciatic nerve transection model reported that WJ-MSCs have greater peripheral nerve regeneration abilities than ASCs [3]. Yet, studies on the mechanism of SCLCs derived from WJ-MSCs are insufficient, and no study has been conducted to evaluate the degree of peripheral nerve regeneration by application of human WJ-SCLCs using acellular nerve grafts (ANGs) in an *in vivo* rat model. We prepared ANGs using a new protocol developed and patented by our laboratory (PCT/KR2019/005966) [29], in which the cells are completely removed and the extracellular matrix structures of the nerves are maintained. Particularly, ANGs are promising in this area because they have a low immune rejection response and exhibit more effective sciatic nerve

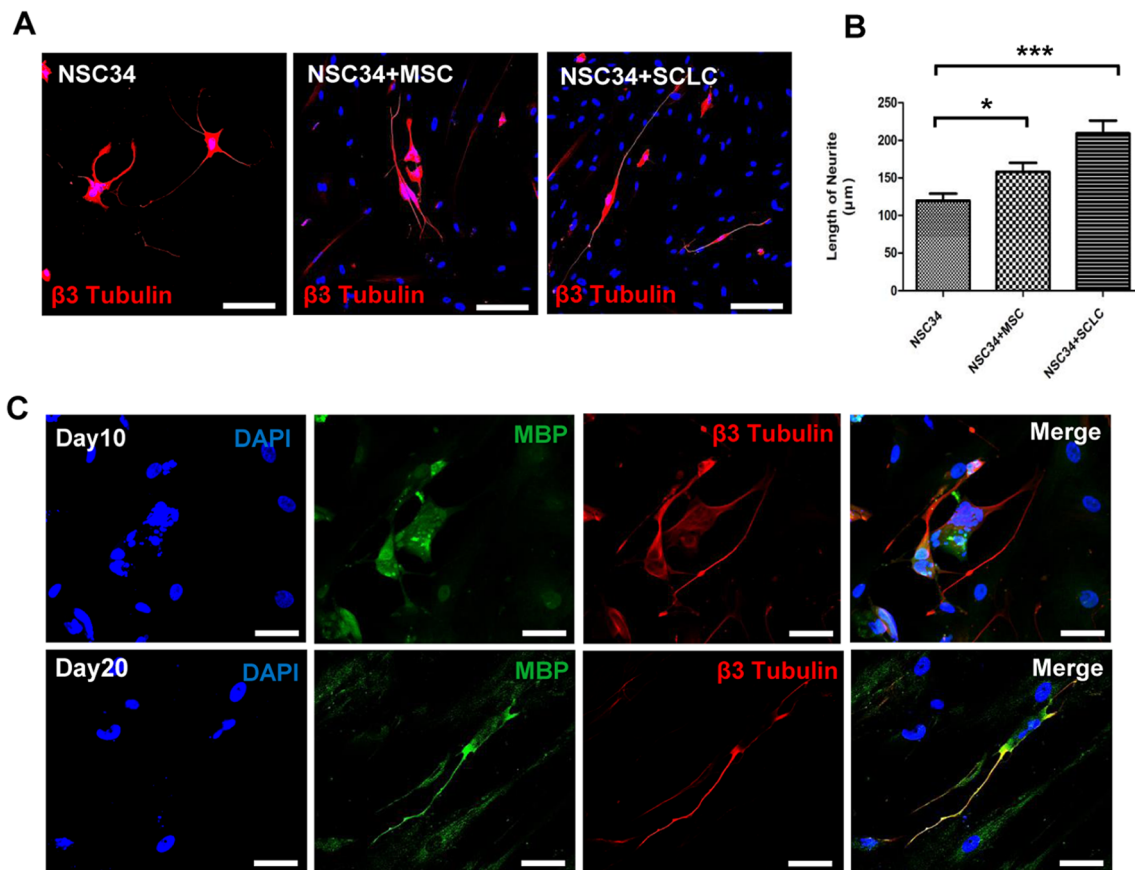


Fig. 4 Neurite outgrowth and myelination in NSC34 cells co-cultured with WJ-MSCs and SCLCs. **A** Immunofluorescence staining for β -III tubulin in NSC34 cells cultured alone or after co-culture for 7 days with WJ-MSCs, and WJ-SCLCs. Scale bar = 200 μ m.

B Length of the longest neurite in each group. Results are shown as mean \pm SEM (* p < 0.05, *** p < 0.001). **C** Co-immunofluorescence staining of MBP and β -III tubulin for myelination for 10 and 20 days with NSC34 cells and WJ-MSCs. Scale bar = 50 μ m

regeneration effects than conventional nerve conduits [5, 38]. However, ANGs alone are limited in promoting long-term axon regeneration, and neuro-supporting cells such as Schwann cells are required for adequate axon proliferation. As autologous Schwann cells augment myelination in peripheral nerve injuries and may thus accelerate the generation of peripheral nerves [39], we assumed that the WJ-SCLCs-laden ANGs could promote peripheral nerve regeneration in an animal model. Therefore, we investigated the potential of WJ-SCLCs as an alternative to SCs.

We first demonstrated that WJ-MSCs isolated from human umbilical cords have the capacity to differentiate into Schwann cell-like cells in terms of phenotype and surface marker expression. WJ-MSCs cultured in our laboratory showed that they possessed the differentiation potential characteristic of MSCs (CD73⁺ CD105⁺ CD45⁻ CD14⁻). Moreover, after induction with glial growth factors (heregulin, bFGF, PDGF, and forskolin), the phenotype of WJ-MSCs changed from fibroblast-like

morphology to a spindle-like shape, similar to that of Schwann cells.

SCs have various stages of development, and each stage has specific markers [40]. During the development of SCs, mature SCs are further divided into myelinated and non-myelinated types [34]. Particularly, GFAP appears relatively late in the development process, and is found in non-myelinated Schwann cells. NGFR is also expressed in immature Schwann cells and non-myelinated Schwann cells. S100 β , a widely used SC marker, is expressed in mature Schwann cells and not in Schwann cell precursors. KROX20 is known to suppress the immature state and induce myelination, and myelin basic protein (MBP) is a specific marker of the mature stage of the development of SCs [33, 41–44]. Therefore, we compared the expression of SC-specific markers in differentiated-SCLCs with that in undifferentiated-MSCs using real-time PCR, Western Blot analysis, and immunocytochemical staining; as a result, we observed that WJ-SCLCs had stronger expression levels of S100 β , GFAP, NGFR, and KROX20 than did WJ-MSCs. Collectively, the increased levels of these markers in WJ-

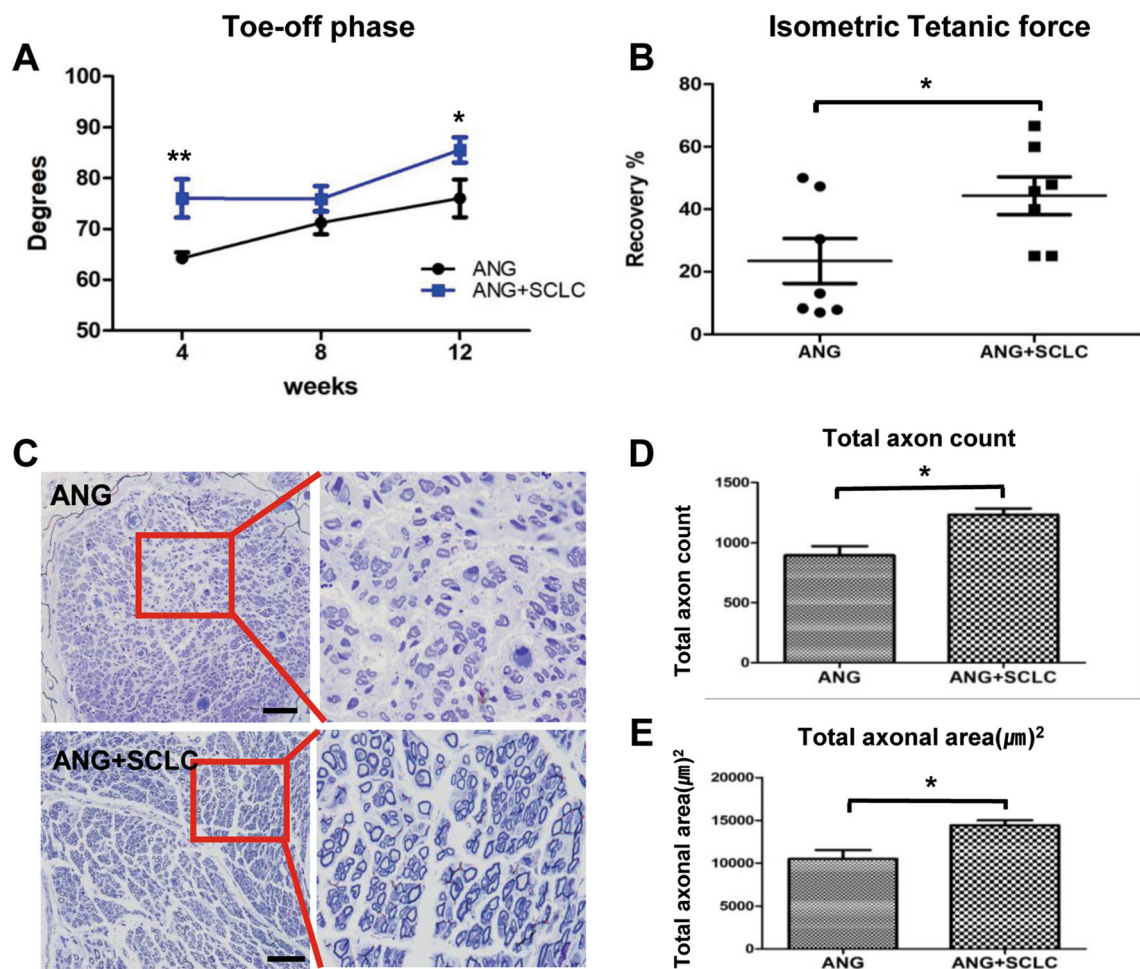


Fig. 5 *In vivo* functional recovery. **A** Analysis of video gait angles at the toe-off phase. The angles were measured in control and WJ-SCLCs groups for up to 12 weeks following transplantation surgery. **B** Measurement of the isometric tetanic force at the recovery rate at post-operative 16 weeks. **C** Microscopic examination of toluidine blue-stained distal sciatic nerve ends at post-operative 16 weeks,

showing the histological structures of nerve fiber, axon, and myelin. Scale bar = 50 μm. **D**, **E** Total axon count and total axonal area are shown. The mean ± SEM of the ANG only control group and the WJ-SCLCs-laden ANG groups are compared ($*p < 0.05$, Student's *t*-test)

SCLCs indicate that MSCs can readily differentiate into mature Schwann cell-like cells and not into Schwann cell precursors in the early stages of differentiation.

Mature SCs support the growth of axons by secreting a variety of neurotrophic factors such as GDNF, FGF, and BDNF [1, 12]. Therefore, we investigated whether WJ-SCLCs also secreted neurotrophic factors using the Neuro Discovery array. As a result, we observed that compared with WJ-MSCs, WJ-SCLCs had significantly higher levels of growth factors such as BDNF, GDNF, and G-CSF. Neurotrophic factors stimulate the outgrowth of neurites and enhance the differentiation and proliferation of neuronal cells [45, 46]. BDNF regulates axonal regeneration by activating the PI3K-AKT and MEK-ERK1/2 pathways [47]. GDNF enhances axonal regeneration and myelination by promoting the survival and proliferation of Schwann cells [48]. G-CSF is a well-known glycoprotein that

stimulates the bone marrow to produce granulocytes and stem cells and secretes molecules involved in the proliferation and differentiation of hematopoietic progenitor cells [49]; moreover, G-CSF exerts neuroprotective effects through different mechanisms including anti-apoptosis, anti-inflammation, neuronal differentiation, and angiogenesis [50]. In the present study, we demonstrated that these factors secreted from WJ-SCLCs might play important roles in enhancing neurite outgrowth and modify the surrounding conditions of ANGs for sciatic nerve regeneration.

We also investigated the role of WJ-SCLCs on neurite outgrowth and myelination using a co-culture system and found that similar to SCs, WJ-SCLCs effectively enhanced neurite outgrowth and induced MBP expression. NSC34 cells have been shown to express neurotrophic factor receptors such as p75NTR and tyrosine kinase receptor B

(TrkB) [28, 51, 52]; therefore, it is plausible that neurotrophic factors secreted from WJ-SCLCs can promote the outgrowth of neurites by interacting with the receptors on NSC34 cells, indicating that WJ-SCLCs are a viable alternative to native SCs.

We also carried out video gait and isometric tetanic force analysis to investigate the role of WJ-SCLCs on *in vivo* functional recovery, and found that implantation of WJ-SCLCs-laden ANGs significantly improved the peripheral nerve regeneration in a rat model compared with CTL, thereby strongly suggesting that WJ-SCLCs can support axon outgrowth and structural formation of myelin sheaths in peripheral nerve injury. Consistent with the functional recovery results, the pattern of toluidine blue staining in the regenerated sciatic nerve indicated that WJ-SCLCs indeed facilitated axonal regrowth and remyelination. As WJ-SCLCs were able to elongate neurite outgrowth during co-culture with NSC34 cells, we inferred that WJ-SCLCs directly improved the gait after nerve injury repair by myelinating the regenerated axons. However, after implantation of WJ-SCLCs ANGs in an injured rat model, human-specific markers such as anti-human nuclear antibodies were initially observed in the implants and not thereafter (data not shown). Nevertheless, the implantation of WJ-SCLCs led to the recovery of peripheral nerves. These results suggest that the signaling factors secreted by WJ-SCLCs recruited the endogenous host SCs to promote myelination, as observed in the spinal cord injury model [53, 54]. The neurotrophic factors secreted from the host SCs might have promoted the regeneration of the peripheral nerves, and the neurotrophic factor secreted by the WJ-SCLCs might also have affected the axonal regeneration of the damaged sciatic nerve. Although damaged peripheral nerve axons have the capability of regrowth, complete functional recovery is difficult [55] because the axon growth cone may be blocked by barriers such as myelin debris, inflammatory cells, and glial cells during regeneration. In addition to their functions regarding myelination and neurotropism, SCs play an important role in the destruction of tissue debris at the site of injury and provides a nutrient environment for nerve regeneration [56–58]. Therefore, considering these various roles of SCs, it can be inferred that WJ-SCLCs can also induce functional improvement in peripheral nerve repair.

Some similar studies have been published on this issue. Peng et al. conducted an *in vitro* experiment using SCLCs differentiated from WJ-MSCs [59], but did not further investigate the usefulness of SCLCs using *in vivo* models. Pereira et al. investigated the potential of poly(DL-lactide- ϵ -caprolactone) (PLC) membranes for inducing nerve regeneration in an animal model [60] and showed promising results. However, PLC membrane conduits are limited in that they do not have extracellular matrix

structures, whereas ANGs retain the internal structures as well as the extracellular matrix structures for guiding cell migration and nerve fiber elongation. [29] Lastly, Jung et al. showed that tonsil-derived MSCs, a novel source of MSCs, were effective in ameliorating peripheral nerve scarring [19]. However, as Jung et al. used a relatively mild injury model, additional investigation in models with more severe injuries is warranted.

Our study is limited in that the *in vivo* experiments did not include a sham negative control group (injury only) and an ANG + WJ-MSC group, which would have been useful for comparison with the ANG and ANG + WJ-SCLCs groups in our study. Despite this limitation, however, this is the first study to apply WJ-SCLCs to ANGs for peripheral nerve regeneration *in vivo*, and our results showed that WJ-SCLCs-laden ANGs significantly outperformed ANGs alone in sciatic nerve regeneration.

In summary, our results show that WJ-MSCs have the ability to differentiate into WJ-SCLCs that effectively enhance the outgrowth of neurites *in vitro*. In addition, implantation of WJ-SCLCs-laden ANGs were superior to ANGs alone in inducing functional recovery after sciatic nerve injury. WJ-MSCs may serve as a valuable source of SCs for use in transplantation, and human WJ-SCLCs may be effective for promoting the regeneration of peripheral nerves.

Acknowledgements We thank the Stem Cell Institute at Asan Medical Center for providing the WJ-MSCs and the Electron Microscopy core facility at the Convergence mEDicine research cenTer (CREDIT) for support and instrumentation. This study was supported by a grant from Asan Institute for Life Sciences, Asan Medical Center, Republic of Korea (#2019IP0766-1, 2020IP0079-1) and by the National Research Foundation of Korea (NRF-2017R1A2B4003692, 2020R1A2C1006656), funded by the Ministry of Science, ICT, and Future Planning.

Compliance with ethical standards

Conflict of interest The authors have declared that there is no conflict of interest.

Ethical statement The study protocol was approved by the Asan Medical Center Institutional Review Board (#2015-0303), which waived the need for informed consent. All animal studies were performed after receiving approval from the Institutional Animal Care and Use Committee at Asan Medical Center (#2017-12-127).

References

1. He B, Zhu Z, Zhu Q, Zhou X, Zheng C, Li P, et al. Factors predicting sensory and motor recovery after the repair of upper limb peripheral nerve injuries. *Neural Regen Res.* 2014;9:661–72.
2. Li R, Liu Z, Pan Y, Chen L, Zhang Z, Lu L. Peripheral nerve injuries treatment: a systematic review. *Cell Biochem Biophys.* 2014;68:449–54.

3. Wang AYL, Loh CYY, Shen HH, Hsieh SY, Wang IK, Chuang SH, et al. Topical application of human Wharton's jelly mesenchymal stem cells accelerates mouse sciatic nerve recovery and is associated with upregulated neurotrophic factor expression. *Cell Transplant*. 2019;28:1560–72.
4. Vanderhooft E. Functional outcomes of nerve grafts for the upper and lower extremities. *Hand Clin*. 2000;16:93–104, ix.
5. Fan L, Yu Z, Li J, Dang X, Wang K. Schwann-like cells seeded in acellular nerve grafts improve nerve regeneration. *BMC Musculoskelet Disord*. 2014;15:165.
6. Philips C, Cornelissen M, Carriel V. Evaluation methods as quality control in the generation of decellularized peripheral nerve allografts. *J Neural Eng*. 2018;15:021003.
7. Johnson PJ, Newton P, Hunter DA, Mackinnon SE. Nerve endoneurial microstructure facilitates uniform distribution of regenerative fibers: a post hoc comparison of midgraft nerve fiber densities. *J Reconstr Microsurg*. 2011;27:83–90.
8. Whitlock EL, Tuffaha SH, Luciano JP, Yan Y, Hunter DA, Magill CK, et al. Processed allografts and type I collagen conduits for repair of peripheral nerve gaps. *Muscle Nerve*. 2009;39:787–99.
9. Brenner MJ, Lowe JB 3rd, Fox IK, Mackinnon SE, Hunter DA, Darcy MD, et al. Effects of Schwann cells and donor antigen on long-nerve allograft regeneration. *Microsurgery*. 2005;25:61–70.
10. Nagarajan R, Le N, Mahoney H, Araki T, Milbrandt J. Deciphering peripheral nerve myelination by using Schwann cell expression profiling. *Proc Natl Acad Sci U S A*. 2002;99:8998–9003.
11. Iwase T, Jung CG, Bae H, Zhang M, Soliven B. Glial cell line-derived neurotrophic factor-induced signaling in Schwann cells. *J Neurochem*. 2005;94:1488–99.
12. Monk KR, Feltri ML, Taveggia C. New insights on Schwann cell development. *Glia*. 2015;63:1376–93.
13. Jessen KR, Mirsky R. The repair Schwann cell and its function in regenerating nerves. *J Physiol*. 2016;594:3521–31.
14. Amé-Thomas P, Maby-El Hajjami H, Monvoisin C, Jean R, Monnier D, Caulet-Maugendre S, et al. Human mesenchymal stem cells isolated from bone marrow and lymphoid organs support tumor B-cell growth: role of stromal cells in follicular lymphoma pathogenesis. *Blood*. 2007;109:693–702.
15. Williams AR, Hare JM. Mesenchymal stem cells: biology, pathophysiology, translational findings, and therapeutic implications for cardiac disease. *Circ Res*. 2011;109:923–40.
16. Saulite L, Vavers E, Zvejniece L, Dambrova M, Riekstina U. The differentiation of skin mesenchymal stem cells towards a Schwann cell phenotype: impact of sigma-1 receptor activation. *Mol Neurobiol*. 2018;55:2840–50.
17. Reid AJ, Sun M, Wiberg M, Downes S, Terenghi G, Kingham PJ. Nerve repair with adipose-derived stem cells protects dorsal root ganglia neurons from apoptosis. *Neuroscience*. 2011;199:515–22.
18. Ladak A, Olson J, Tredget EE, Gordon T. Differentiation of mesenchymal stem cells to support peripheral nerve regeneration in a rat model. *Exp Neurol*. 2011;228:242–52.
19. Jung N, Park S, Choi Y, Park JW, Hong YB, Park HH, et al. Tonsil-derived mesenchymal stem cells differentiate into a schwann cell phenotype and promote peripheral nerve regeneration. *Int J Mol Sci*. 2016;17:1867.
20. Bajada S, Mazakova I, Richardson JB, Ashammakhi N. Updates on stem cells and their applications in regenerative medicine. *J Tissue Eng Regen Med*. 2008;2:169–83.
21. Fong CY, Chak LL, Biswas A, Tan JH, Gauthaman K, Chan WK, et al. Human Wharton's jelly stem cells have unique transcriptome profiles compared to human embryonic stem cells and other mesenchymal stem cells. *Stem Cell Rev Rep*. 2011;7:1–16.
22. El Omar R, Beroud J, Stoltz JF, Menu P, Velot E, Decot V. Umbilical cord mesenchymal stem cells: the new gold standard for mesenchymal stem cell-based therapies? *Tissue Eng Part B Rev*. 2014;20:523–44.
23. Barrett AN, Fong CY, Subramanian A, Liu W, Feng Y, Choolani M, et al. Human Wharton's jelly mesenchymal stem cells show unique gene expression compared with bone marrow mesenchymal stem cells using single-cell RNA-sequencing. *Stem Cells Dev*. 2019;28:196–211.
24. Kim W, Lee SK, Kwon YW, Chung SG, Kim S. Pioglitazone-primed mesenchymal stem cells stimulate cell proliferation, collagen synthesis and matrix gene expression in tenocytes. *Int J Mol Sci*. 2019;20:472.
25. Xu Y, Liu L, Li Y, Zhou C, Xiong F, Liu Z, et al. Myelin-forming ability of Schwann cell-like cells induced from rat adipose-derived stem cells in vitro. *Brain Res*. 2008;1239:49–55.
26. Pfaffl MW. A new mathematical model for relative quantification in real-time RT-PCR. *Nucleic Acids Res*. 2001;29:e45.
27. Choi SJ, Cho AR, Jo SJ, Hwang ST, Kim KH, Kwon OS. Effects of glucocorticoid on human dermal papilla cells in vitro. *J Steroid Biochem Mol Biol*. 2013;135:24–9.
28. Takaku S, Yako H, Niimi N, Akamine T, Kawanami D, Utsunomiya K, et al. Establishment of a myelinating co-culture system with a motor neuron-like cell line NSC-34 and an adult rat Schwann cell line IFRS1. *Histochem Cell Biol*. 2018;149:537–43.
29. Shin YH, Park SY, Kim JK. Comparison of systematically combined detergent and nuclease-based decellularization methods for acellular nerve graft: an ex vivo characterization and in vivo evaluation. *J Tissue Eng Regen Med*. 2019;13:1241–52.
30. Zhao Z, Wang Y, Peng J, Ren Z, Zhang L, Guo Q, et al. Improvement in nerve regeneration through a decellularized nerve graft by supplementation with bone marrow stromal cells in fibrin. *Cell Transplant*. 2014;23:97–110.
31. Lee JY, Giusti G, Wang H, Friedrich PF, Bishop AT, Shin AY. Functional evaluation in the rat sciatic nerve defect model: a comparison of the sciatic functional index, ankle angles, and isometric tetanic force. *Plast Reconstr Surg*. 2013;132:1173–80.
32. Sun X, Zhu Y, Yin HY, Guo ZY, Xu F, Xiao B, et al. Differentiation of adipose-derived stem cells into Schwann cell-like cells through intermittent induction: potential advantage of cellular transient memory function. *Stem Cell Res Ther*. 2018;9:133.
33. Decker L, Desmarquet-Trin-Dinh C, Taillebourg E, Ghislain J, Vallat JM, Charnay P. Peripheral myelin maintenance is a dynamic process requiring constant Krox20 expression. *J Neurosci*. 2006;26:9771–9.
34. Liu Z, Jin YQ, Chen L, Wang Y, Yang X, Cheng J, et al. Specific marker expression and cell state of Schwann cells during culture in vitro. *PLoS One*. 2015;10:e0123278.
35. Shin RH, Vathana T, Giessler GA, Friedrich PF, Bishop AT, Shin AY. Isometric tetanic force measurement method of the tibialis anterior in the rat. *Microsurgery*. 2008;28:452–7.
36. Cooney DS, Wimmers EG, Ibrahim Z, Grahmmer J, Christensen JM, Brat GA, et al. Mesenchymal stem cells enhance nerve regeneration in a rat sciatic nerve repair and hindlimb transplant model. *Sci Rep*. 2016;6:31306.
37. Faroni A, Rothwell SW, Grolla AA, Terenghi G, Magnaghi V, Verkhatsky A. Differentiation of adipose-derived stem cells into Schwann cell phenotype induces expression of P2X receptors that control cell death. *Cell Death Dis*. 2013;4:e743.
38. Wang D, Liu XL, Zhu JK, Jiang L, Hu J, Zhang Y, et al. Bridging small-gap peripheral nerve defects using acellular nerve allograft implanted with autologous bone marrow stromal cells in primates. *Brain Res*. 2008;1188:44–53.
39. Chalfoun CT, Wirth GA, Evans GR. Tissue engineered nerve constructs: where do we stand? *J Cell Mol Med*. 2006;10:309–17.
40. Jessen KR, Mirsky R. The origin and development of glial cells in peripheral nerves. *Nat Rev Neurosci*. 2005;6:671–82.

41. Jessen KR, Brennan A, Morgan L, Mirsky R, Kent A, Hashimoto Y, et al. The Schwann cell precursor and its fate: a study of cell death and differentiation during gliogenesis in rat embryonic nerves. *Neuron*. 1994;12:509–27.
42. Yu WM, Yu H, Chen ZL, Strickland S. Disruption of laminin in the peripheral nervous system impedes nonmyelinating Schwann cell development and impairs nociceptive sensory function. *Glia*. 2009;57:850–9.
43. Jung J, Cai W, Jang SY, Shin YK, Suh DJ, Kim JK, et al. Transient lysosomal activation is essential for p75 nerve growth factor receptor expression in myelinated Schwann cells during Wallerian degeneration. *Anat Cell Biol*. 2011;44:41–9.
44. Triolo D, Dina G, Lorenzetti I, Malaguti M, Morana P, Del Carro U, et al. Loss of glial fibrillary acidic protein (GFAP) impairs Schwann cell proliferation and delays nerve regeneration after damage. *J Cell Sci*. 2006;119:3981–93.
45. Skaper SD. Neurotrophic factors: an overview. *Methods Mol Biol*. 2018;1727:1–17.
46. Skaper SD. The neurotrophin family of neurotrophic factors: an overview. *Methods Mol Biol*. 2012;846:1–12.
47. Shih CH, Chen CJ, Chen L. New function of the adaptor protein SH2B1 in brain-derived neurotrophic factor-induced neurite outgrowth. *PLoS One*. 2013;8:e79619.
48. Hwang K, Jung K, Kim IS, Kim M, Han J, Lim J, et al. Glial cell line-derived neurotrophic factor-overexpressing human neural stem/progenitor cells enhance therapeutic efficiency in rat with traumatic spinal cord injury. *Exp Neurobiol*. 2019;28:679–96.
49. Deotare U, Al-Dawsari G, Couban S, Lipton JH. G-CSF-primed bone marrow as a source of stem cells for allografting: revisiting the concept. *Bone Marrow Transplant*. 2015;50:1150–6.
50. Lu CZ, Xiao BG. G-CSF and neuroprotection: a therapeutic perspective in cerebral ischaemia. *Biochem Soc Trans*. 2006;34:1327–33.
51. Matusica D, Fenech MP, Rogers ML, Rush RA. Characterization and use of the NSC-34 cell line for study of neurotrophin receptor trafficking. *J Neurosci Res*. 2008;86:553–65.
52. Sabitha KR, Sanjay D, Savita B, Raju TR, Laxmi TR. Electrophysiological characterization of Nsc-34 cell line using micro-electrode Array. *J Neurol Sci*. 2016;370:134–9.
53. Biernaskie J, Sparling JS, Liu J, Shannon CP, Plemel JR, Xie Y, et al. Skin-derived precursors generate myelinating Schwann cells that promote remyelination and functional recovery after contusion spinal cord injury. *J Neurosci*. 2007;27:9545–59.
54. Sparling JS, Bretzner F, Biernaskie J, Assinck P, Jiang Y, Arisato H, et al. Schwann cells generated from neonatal skin-derived precursors or neonatal peripheral nerve improve functional recovery after acute transplantation into the partially injured cervical spinal cord of the rat. *J Neurosci*. 2015;35:6714–30.
55. Walsh S, Midha R. Practical considerations concerning the use of stem cells for peripheral nerve repair. *Neurosurg Focus*. 2009;26:E2.
56. Gaudet AD, Popovich PG, Ramer MS. Wallerian degeneration: gaining perspective on inflammatory events after peripheral nerve injury. *J Neuroinflammation*. 2011;8:110.
57. Dubový P, Jančálek R, Kubek T. Role of inflammation and cytokines in peripheral nerve regeneration. *Int Rev Neurobiol*. 2013;108:173–206.
58. Jessen KR, Mirsky R. The success and failure of the Schwann cell response to nerve injury. *Front Cell Neurosci*. 2019;13:33.
59. Peng J, Wang Y, Zhang L, Zhao B, Zhao Z, Chen J, et al. Human umbilical cord Wharton's jelly-derived mesenchymal stem cells differentiate into a Schwann-cell phenotype and promote neurite outgrowth in vitro. *Brain Res Bull*. 2011;84:235–43.
60. Pereira T, Gärtner A, Amorim I, Almeida A, Caseiro AR, Armada-da-Silva PA, et al. Promoting nerve regeneration in a neurotmesis rat model using poly(DL-lactide-epsilon-caprolactone) membranes and mesenchymal stem cells from the Wharton's jelly. In vitro and in vivo analysis. *Biomed Res Int*. 2014;2014:302659.

Publisher's Note Springer Nature remains neutral with regard to jurisdictional claims in published maps and institutional affiliations.